JOURNAL OF COMPUTATIONAL PHYSICS 67, 188–213 (1986)

An Adaptive Characteristic Petrov–Galerkin Finite Element Method for Convection-Dominated Linear and Nonlinear Parabolic Problems in One Space Variable

L. DEMKOWICZ AND J. T. ODEN

The Texas Institute for Computational Mechanics,
Department of Aerospace Engineering and Engineering Mechanics,
The University of Texas at Austin, Austin, Texas

Received June 5, 1985; revised March 5, 1986

A new adaptive finite element method for convection-dominated problems is presented. A special feature of the method is that it is based on a Petrov–Galerkin scheme for spatial approximation at a typical time-step which employs test functions chosen so that the approximate solution coincides with the exact solution at the nodes of finite element grid. This procedure makes possible the derivation of *truly local* a posteriori error estimates and a very effective solver. Numerical examples are discussed which illustrate the efficiency and effectively of the method. © 1986 Academic Press, Inc.

1. INTRODUCTION

In the present paper, we present a new adaptive finite element method for convection-dominated problems in one space variable with small but constant viscosity. Among special features of our results, we mention the calculation of optimal test functions for given piecewise linear trial functions, the establishment of what we call "extrasuperconvergence" results for certain elliptic problems (by which we mean that the approximation is exact at nodal points), the establishment of truly local a posteriori estimates in the L^2-, energy-, and L^∞-norms, the merger of the method of characteristics with special Petrov–Galerkin concepts, and applications to representative linear and nonlinear parabolic and hyperbolic problems. We mention that other adpative dinite element schemes for linear parabolic problems have been proposed in the important papers of Bietermann and Babuska [5, 6, 7] and Bietermann [4].

Following the Introduction, we develop a special characteristic Petrov–Galerkin (CPG) method for solving the linear convection dominated diffusion problem (see (2.1)) with a small, but constant diffusion coefficient, ε.

The method involves two steps. First, we utilize a method of charactistics and discretizations in time to replace the original equation by a sequence of

0021-9991/86 $3.00

corresponding elliptic problems. Next, we develop a special Petrov–Galerkin method for treating the typical "elliptic step." We make use of the concept of optimal test functions, as suggested by Barret and Morton [3]. While these authors used such functions to symmetrize nonsymmetric problems, our elliptic problem is symmetric from the start, so that the philosophy behind our use of optimal test functions is to change the norm in which the convergence of standard Bubnov–Galerkin method takes place, to one which is better from a computational point of view. In particular, we devise new test functions which exhibit a very important feature: they force the coincidence of the approximate and exact solutions at finite element nodes. This important feature of our method allows us to derive *truly local a posteriori error estimates* and results in a very effective elliptic solver.

It is known (see, e.g., Babuska and Rheinboldt [1, 2] and Szymczak and Babuska [17, 18]) that if nodal errors are nearly zero, local a posteriori error estimates can be derived which serve as a basis for effective adaptive schemes, and this fact is exploited in the present work.

The success of the concept of the optimal test functions lies in the fact that they can be defined as linear combinations of local shape functions; i.e., shape functions with support contained within two adjacent elements. These localized test functions are very similar to those, e.g., in Szymczak and Babuska [17, 18], or Hughes [12], but the way we obtain them is quite different.

Our combination of the method of characteristics with the adaptive Petrov–Galerkin scheme generalizes the works of, e.g., Pironneau [15], Douglas and Russell [10], or Huffenus and Khaletzky [11] devoted to characteristic *Bubnov–Galerkin* schemes. Let us also note that the method of lines we employ is quite different from the classical one: *first*, we discretize the evolution problem with respect to time, and then deal with the typical elliptic step. This allows us, in particular, to use an adaptive strategy in obtaining very good numerical solutions.

In Section 3 of this paper, issues of numerical integration and L^2-instability bring us to a study of what we refer to as *numerically optimal test functions*. More precisely, we study a version of our method which can be considered as a very special solver to the system of equations resulting from the characteristic Bubnov–Galerkin method. The concept allows us to resolve difficulties connected with stability and turns out to provide for a very effective basis for application of our method to cases involving moderately small diffusion parameters ε.

The method we present is motivated by a preliminary study of compressible-viscous flows and as an initial step toward treating such problems, we present in Section 4 a study of nonlinear parabolic problems with small diffusion resulting from a parabolic regularization of one-dimensional hyperbolic conservation laws.

We conclude the paper with discussions of results of numerical experiments in Section 5 and some final remarks in Section 6.

2. Convection-Dominated Linear Diffusion Problems in One Space Variable—The Adaptive Characteristic Petrov–Galerkin Finite Element Method

The goal of this paper is to develop an adaptive finite element method for solving the following class of convection-dominated diffusion problems:

Find $u = u(x, t)$ such that

$$\begin{aligned} &u_t + cu_x - \varepsilon u_{xx} = f, && (x, t) \in (0, 1) \times (0, T), \\ &u(0, t) = a(t);\ u(1, t) = b(t), && t \in (0, T), \\ &u(x, 0) = u_0(x), && x \in (0, 1). \end{aligned} \tag{2.1}$$

Here ε is a "small" positive number ($\varepsilon \ll |c|$), $c = c(x, t)$ is a given transport function; $a(t)$, $b(t)$, and $u_0(x)$ are boundary and initial data, respectively, and $f = f(x, t)$ is a given source term; for the moment, all these data are assumed to be smooth function of their arguments.

The discussion of our method for (2.1) is divided into four parts:

(1) An approximation of the original problem by a series of symmetric elliptic problems by a method of characteristics.

(2) An analysis of a typical elliptic step in the process, including in particular a discussion of a Petrov–Galerkin method with optimal test functions.

(3) The development of a posteriori local error estimates and a discussion of an adaptive finite element procedure.

(4) The combination of the adaptive finite element method with the method of characteristics resulting in the new method and the corresponding a priori error analysis.

2.1. *Reduction to a System of Elliptic Problems*

One common method of approximating (2.1) is the classical "method of lines." Traditionally, this method involves the construction of a finite element approximation with respect to the space variable x, thus turning (2.1) into a system of ordinary differential equations in time, and then the solution of the system using any appropriate ODE solver. In our approach, we follow an opposite tack, approximating (2.1) *first* with respect to time and then analyzing the typical elliptic step.

We begin by introducing a partition of interval $(0, T)$ with nodes:

$$0 = t_0 < t_1 < \cdots < t_K = T \tag{2.2}$$

and then we replace (2.1) by the following sequence of elliptic problems:

For each $k = 1,..., K$, find $w^k(x)$ such that

$$\begin{aligned} &w^k - \varepsilon\, \Delta t w^k_{xx} = f(x, t_k)\, \Delta t + w^{k-1}(X(x, t_k; t_{k-1})), \\ &w^k(0) = a(t^k),\ w^k(1) = b(t^k). \end{aligned} \tag{2.3}$$

Here $\Delta t = \Delta t_k = t_k - t_{k-1}$, $w^{k-1} = w(x, (k-1)\,\Delta t)$ for $k > 1$ and $w^{k-1} = u_0(x)$ for $k = 1$, and $X(x, t_k; \cdot)$ is the characteristic line drawn backward in time the point (x, t_k). More precisely, $X(x, t)$ is the solution of the ordinary differential equation:

$$\begin{aligned} &\frac{dX}{d\tau} = c(X, \tau), \\ &X(t) = x. \end{aligned} \tag{2.4}$$

If $c(x, t)$ is continuous and Lipschitz continuous with respect to x, then such characteristic lines exist for every time τ and one and only one characteristic passes through each point (x, t).

In implementing (2.3), we shall view it as a fractional-step method of the type:

$$\begin{aligned} &\frac{Dw^{k-(1/2)}}{Dt} = 0, \\ &\frac{w^k - w^{k-(1/2)}}{\Delta t} - \varepsilon w^k_{xx} = f, \end{aligned} \tag{2.5}$$

where D/Dt is the (absolute) derivative in the direction of the characteristic line. Thus, the solution at the conclusion of a time-step is computed as the sum of a pure convection component and a diffusive part.

Remark 2.1. Note that the source term in (2.5) is first switched off and then applied in its entirety only at the diffusion step. An opposite scheme would result if we had replaced the homogeneous pure convection step (resulting in $(2.5)_1$) by the inhomogeneous equation,

$$u_t + cu_x = f. \tag{2.6}$$

In such a case, the solution $w^{k-(1/2)}(x) = w^{k-1}(X(x, t_k; t_{k-1}))$ would have to be replaced by the function:

$$w^{k-(1/2)}(x) = w^{k-1}(X(x, t_k; t_{k-1})) + \int_{t_{k-1}}^{t_k} f(X(x, t_k; \tau)_1\, \tau)\, d\tau. \tag{2.7}$$

This would result in an algorithm of the form (2.3) with $f(x, t_k)\, \Delta t$ replaced by

$$\int_{t_{k-1}}^{t_k} f(X(x, t_k; \tau), \tau)\, d\tau. \tag{2.8}$$

Clearly, these two schemes coincide only when f is independent of time and $c \equiv 0$. An alternative might be to split f into two parts, each contributing to one or the other fractional steps. Such decompositions are often impossible or, at best, impractical, and we shall follow Pironneau [15] and employ the first "convective-diffusion" scheme.

2.2. *Bubnov and Petrov–Galerkin Finite Element Methods for the Elliptic Problem*

Before we turn to a study of the elliptic problem (2.3), we record some standard results concerning the classical finite element method applied to the simplest elliptic problem:

Find u: $(0, 1) \mapsto \mathbb{R}$ such that

$$\begin{aligned} -u_{xx} &= f \qquad \text{in } (0, 1), \\ u(0) &= a, \qquad u(1) = b, \end{aligned} \tag{2.9}$$

where $u_{xx} = du(x)/dx^2$. The corresponding variational formulation is:

Find $u \in H^1(0, 1)$ such that

$$\begin{aligned} &\int_0^1 u_x v_x \, dx = \int_0^1 fv \, dx, \qquad \forall v \in H_0^1(0, 1), \\ &u(0) = a, \qquad u(1) = b. \end{aligned} \tag{2.10}$$

Here H^1 and H_0^1 are the usual Sobolev spaces and boundary condition $(2.10)_2$ is meaningful due to the embedding $H^1(0, 1) \subsetneq C^0([0, 1])$.

The standard Bubnov–Galerkin finite element method with C^0-piecewise linear approximation can be introduced as follows:

Given a subdivision,

$$0 = x_0 < x_1 < \cdots < x_{N-1} < x_N = 1 \tag{2.11}$$

we associate with each node x_i a global basis function ψ_i defined setting:

$$\begin{aligned} &-\psi_{i\,xx} = 0 \qquad \text{in } (x_{i-1}, x_i), \; i = 1, \ldots, N, \\ &\psi_i(x_j) = \delta_{ij}. \end{aligned} \tag{2.12}$$

Such a standard "hat function" is shown in Fig. 1.

By replacing u and v in (2.10) by linear combinations of ψ_i we arrive at the standard Bubnov–Galerkin finite element approximation:

Find $u_h = \sum_{i=0}^{N} u_i \psi_i$ such that

$$\begin{aligned} &\int_0^1 u_{hx} v_{hx} \, dx = \int_0^1 f v_h \, dx, \qquad \forall v_h = \sum_{i=1}^{N-1} v_i \psi_i, \\ &u_0 = a, \qquad u_N = b \quad (v_i = v_h(x_i)). \end{aligned} \tag{2.13}$$

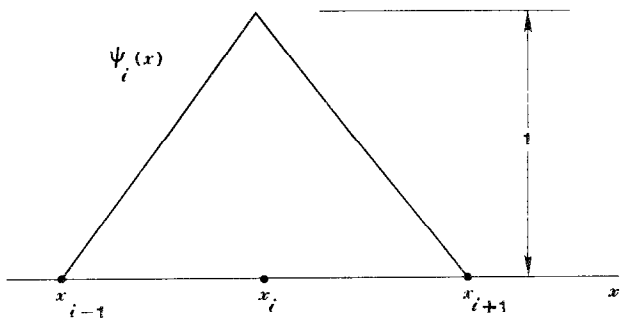

FIG. 1. Standard hat function ψ_i is the solution of the boundary-value problem (2.4).

Let us denote by V_{vh} the finite-dimensional subspace of $H_0^1(0, 1)$ spanned by ψ_i, $i = 1,..., N-1$ and by M_h its affine translation containing functions which satisfy the boundary conditions $(2.13)_2$. By subtracting (2.13) from (2.10) we get the usual condition of orthogonality of the error to V_h,

$$\int_0^1 (u-u_h)_x v_{hx}\, dx = 0, \qquad \forall v_h \in V_h. \tag{2.14}$$

Orthogonality condition (2.14) has two immediate, very important consequences. It yields the *optimal error estimate* (with unit constant):

$$\|u-u_h\| \leqslant \|u-v_h\|, \qquad \forall v \in V_h, \tag{2.15}$$

where $\|\cdot\|$ is the "natural" energy norm,

$$\|u\|^2 = \int_0^1 u_x^2\, dx$$

and it provides extra-super convergence at nodes:

$$u_i = u(x_i) \tag{2.16}$$

i.e., the finite element approximation coincides with the exact solution at the nodes! (cf. Strang and Fix [14]).

Returning now to the elliptic step (2.3), we shall now study the following, slightly more complicated elliptic problem:

Find u: $(0, 1) \mapsto \mathbb{R}$ such that

$$\begin{aligned} &-\varepsilon u_{xx} + u = f, \qquad \varepsilon > 0, \\ &u(0) = a, \qquad u(1) = b. \end{aligned} \tag{2.17}$$

In this problem, ε may represent the product $\varepsilon\, \Delta t$ in (2.3) and f represents the right-hand side in (2.3). Problem (2.17) admits the variational formulation:

Find $u \in H^1(0, 1)$ such that

$$\begin{aligned} &\int_0^1 \varepsilon u_x v_x \, dx + \int_0^1 uv \, dx = \int_0^1 fv \, dx, \qquad \forall v \in H_0^1(0, 1), \\ &u(0) = a, \qquad u(1) = b. \end{aligned} \tag{2.18}$$

By the application of the standard Bubnov–Galerkin finite element method approximation of (2.18) using piecewise linear functions and using the same arguments as before, we again arrive at an orthogonality condition for the error:

$$\varepsilon \int_0^1 (u - u_h)_x v_{hx} \, dx + \int_0^1 (u - u_h) v_h \, dx = 0, \qquad \forall v_h \in V_h. \tag{2.19}$$

Again, (2.19) yields an optimal error estimate, but this time in the different energy norm:

$$\|u\|_E^2 = \varepsilon \int_0^1 u_x^2 \, dx + \int_0^1 u^2 \, dx. \tag{2.20}$$

However, a superconvergence result of the type (2.16) does not hold.

We note that now the energy norm (2.20) consists of basically an L^2-part and a small (ε is implicitly considered to be small) contribution of the H^1-seminorm. In other words, we approach the exact solution at an optimal rate (2.15) but with respect to a nonoptimal choice of a norm. In particular, for cases in which the exact solution u exhibits sharp shock-like transitions, this L^2-type behavior may promote spurious oscillatory behavior in the approximation near such transition regions (wiggles) in much the same manner as Gibb's phenomena in L^2-Fourier analysis. The major question we face at this point is how to avoid these numerical difficulties.

First, we note that the orthogonality condition (2.19) will still be satisfied if we use test functions ϕ_i that are different than the hat functions ψ_i. Let us denote such a new space of test functions of $\hat{V}_h$. Then we obtain the Petrov–Galerkin approximation of (2.18):

Find $u_h \in M_h$ such that

$$\varepsilon \int_0^1 u_{hx} \hat{v}_{hx} \, dx + \int_0^1 u_h \hat{v}_h \, dx = \int_0^1 f \hat{v}_h \, dx, \qquad \forall \hat{v}_h \in \hat{V}_h \tag{2.21}$$

with the corresponding new orthogonality condition,

$$\varepsilon \int_0^1 (u - u_h)_x \hat{v}_{hx} \, dx + \int_0^1 (u - u_h) \hat{v}_h \, dx = 0, \qquad \forall \hat{v}_h \in \hat{V}_h. \tag{2.22}$$

Next for each trial function ψ_i, $i = 1, \ldots, N-1$, we follow the plan of Barret and Morton [1] and define the "optimal" test functions $\hat{v}_i^h$ by solving the problem:

Find $\hat{v}_i^h \in H_0^1(0, 1)$ such that

$$\varepsilon \int_0^1 \phi_x \hat{v}_{ix}^h \, dx + \int_0^1 \phi \hat{v}_i^h \, dx = \int_0^1 \phi_x \psi_{ix} \, dx, \qquad \forall \phi \in H_0^1(0, 1), \tag{2.23}$$

where ψ_i are, again, the hat functions. Before we turn to a deeper study of these so-called optimal test functions $\hat{v}_i^h$, we take note of the remarkable impact they have on the character of our error estimate: By replacing ϕ by the error $u - u_h$ in (2.23) we get

$$\int_0^1 (u - u_h)_x \psi_{ix} \, dx = 0, \qquad i = 1, \ldots, N-1, \ \forall \psi_i, \tag{2.24}$$

which is recognized as our earlier orthogonality condition (2.14). From this fact follow two important properties: (1) an optimal error estimate can now be obtained in a nice norm (particularly one independent of ε), and (2) we obtain an approximation which takes on exact values at the nodes x_i.

We also note that *the optimal test functions are not important in themselves, but rather it is the space they span that is crucial.* In particular, the test functions resulting from (2.23) are *not local* and, therefore, their use in a finite element scheme is of limited practical value. It is, thus, desirable to replace $\hat{v}_i^h$ by other functions, possibly with compact supports, which may either approximate the ideal $\hat{v}_i^h$ well enough or span exactly the space same $\hat{V}_h$.

Toward this end, we define new local test functions ϕ_i, $i = 1, \ldots, N-1$, by the auxiliary problems,

$$\begin{aligned} -\varepsilon \phi_{ixx} + \phi_i &= 0 \qquad \text{in } (x_{i-1}, x_i), \ i = 1, \ldots, N-1, \\ \phi_i(x_j) &= \delta_{ij}, \qquad j = 0, \ldots, N. \end{aligned} \tag{2.25}$$

The following is true:

$$\operatorname{span}\{\phi_i\}_{i=1}^{N-1} = \hat{V}_h \overset{\text{def}}{=} \operatorname{span}\{v_i\}_{i=1}^{N-1}. \tag{2.26}$$

Due to the equal dimensions of spaces V_h and $\hat{V}_h$, it is sufficient to show the inclusion of $\hat{V}_h$ in the left-hand side. Omitting the mesh label h for the moment, let $\hat{v}_i$ denote the optimal (global) test function defined by (2.23) and by $\hat{\hat{v}}_i$ its interpolation of nodes x_i, $i = 1, \ldots, N-1$, obtained using the local test functions ϕ_i, of (2.25); i.e., $\hat{\hat{v}}_i = \sum_j \hat{\hat{v}}_i^j \phi_j(x)$, $\hat{\hat{v}}_i(x_j) = \hat{v}_i(x_j)$, $1 \leqslant i, j \leqslant N-1$. Denoting by w the difference $w(x) = \hat{v}_i(x) - \hat{\hat{v}}_i(x)$, we have

$$\begin{aligned} \varepsilon \int_0^1 w_x^2 \, dx + \int_0^1 w^2 \, dx &= \sum_{i=1}^{N} \int_{x_{i-1}}^{x_i} (\varepsilon w_x w_x + w w) \, dx \\ &= \sum_{i=1}^{N} \int_{x_{i-1}}^{x_i} w(-\varepsilon w_{xx} + w) \, dx = 0, \end{aligned} \tag{2.27}$$

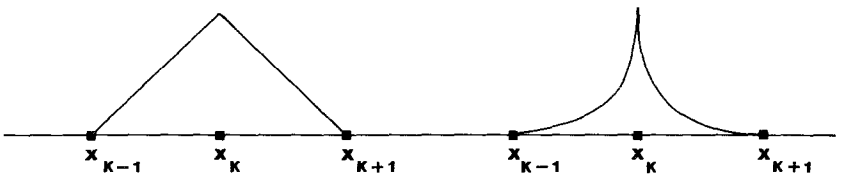

FIG. 2. Trial and optimal test functions.

from which $w \equiv 0$ follows. In this calculation we have used the fact that both $\hat{v}_i$ and ϕ_i satisfy the same homogeneous equation inside every element, ϕ_i from definition (2.25) and $\hat{v}_i$ from (2.23) due to the fact that ψ_i satisfy (2.12)!

The functions ψ_i and ϕ_i are shown in Fig. 2.

In summary, we have developed a strategy for a new class of Petrov–Galerkin finite element methods for (2.17) which exhibit both the optimal-type error estimate (2.15) independent of ε and the superconvergence property (2.16) at nodes. While generalizations to multidimensional cases are not straightforward, they are possible and we plan to report some progress in this direction in a later paper.

An Adaptive Petrov–Galerkin Method in One Dimension. Every adaptive finite element method involves two basic steps:

(1) an a posteriori error estimate

(2) a mesh refinement or enrichment technique.

Virtually all of the a posteriori error estimates used in adaptive schemes proposed in the literature are global in nature, a fact which, nevertheless, has not prevented their use as a basis for local mesh refinements. Contrary to such procedures, the extra-superconvergence result (2.16) allows us to calculate *local error estimates.*

Let $K = (x_{k-1}, x_k)$ be the interior of a typical finite element and let $e^h = u - u_h$ denote the error in the finite element solution. Several local a posteriori error estimates are possible. To derive them, we note that for the model problem (2.17) the error is a solution of the following local boundary value problem:

$$\begin{aligned} -\varepsilon e^h_{xx} + e^h &= f - u_h \qquad \text{in } K, \\ e^h(x_{k-1}) &= e^h(x_k) = 0, \end{aligned} \tag{2.28}$$

where $f - u_h$ is the local element residual. The operator $L\psi = -\varepsilon\psi_{xx} + \psi$ appearing in (2.28) is self-adjoint in $L^2(K)$ and admits a spectral decomposition of the form

$$Lv = -\varepsilon v_{xx} + v = \sum_{i=1}^{\infty} v_i \lambda_j \psi_i, \tag{2.29}$$

where the eigenvalues $\lambda_i = 1 + (\pi^2 i^2 \varepsilon / h^2)$ form an increasing sequence of real numbers, $\psi_i = c_i \sin(\sqrt{(\lambda_i - 1)/\varepsilon}(x - x_{k-1}))$ are the corresponding eigenfunctions which forms an orthonormal basis in $L^2(K)$ (with constants c_i chosen so that $\|\psi_i\|_{L^2} = 1$), $h = x_k - x_{k-1}$ is the mesh size, and v_i are coefficients of the decomposition of a

function v with respect to the basis ψ_i, i.e., $v = \sum_{i=1}^{\infty} v_i \psi_i$. The three norms of major interest associated with L are

$$\|v\|^2_{L^2(K)} = \sum_{i=1}^{\infty} v_i^2,$$

$$\|v\|^2_E = \int (\varepsilon v_x^2 + v^2)\, dx = (Lv, v)_{L^2(K)} = \sum_{i=1}^{\infty} v_i^2 \lambda_i, \tag{2.30}$$

$$\|Lv\|^2_{L^2(K)} = \sum_{i=1}^{\infty} v_i^2 \lambda_i^2.$$

Henceforth we shall assume that $f \in L^2(K)$ so that $\|Lv\|_{L^2(K)}$ in (2.30) is computable for $v = e^h$ and, in fact, this norm is simply the L^2-norm of the residual, $f - u_h$, in $(2.30)_1$. By the direct comparison of the norms, we obtain the following local a posteriori error estimates:

$$\begin{aligned} \|e_h\|_{L^2(K)} &\leqslant \frac{1}{\lambda_1} \|r_h\|_{L^2(K)} \qquad (r_h = f - u_h), \\ \|e_h\|_E &\leqslant (1/\sqrt{\lambda_1})\, \|r_h\|_{L^2(K)}, \qquad \forall K. \end{aligned} \tag{2.31}$$

We emphasize that both of these error estimates are optimal in the sense that there exist functions ϕ for which the equalities hold.

For further development of the method, we will also need estimates in the L^∞-norm, which can be bounded by the energy norm $(2.30)_2$ using the estimate

$$\begin{aligned} u(x) &= \int_{x_{k-1}}^{x} u_x\, dx \qquad (u(x_{k-1}) = 0) \\ &\leqslant \sqrt{x_k - x_{k-1}}\,(1/\sqrt{\varepsilon}) \left(\int_{x_{k-1}}^{x_k} \varepsilon u_x^2\, dx \right)^{1/2}. \\ &\leqslant \left(\frac{h}{\varepsilon} \right)^{1/2} \|u\|_E. \end{aligned} \tag{2.32}$$

Thus, combining this result with $(2.31)_2$, we obtain

$$\|e_h\|_{L^\infty(K)} \leqslant \left[\frac{h^3}{\varepsilon(h^2 + \varepsilon\pi^2)} \right]^{1/2} \|f - u_h\|_{L^2(K)}. \tag{2.33}$$

With this estimate in hand, we now proceed to the second aspect of the mesh refinement technique. Here we propose to use the simplest h-method in its bisectional version. The strategy is outlined as follows:

(1) Choose an initial mesh and solve the system of equations resulting from the Petrov–Galerkin method.

(2) Using estimate (2.33) with a given error tolerance TOL, determine which of the elements need a refinement ($\|e^h\|_{L^\infty(K)} \geqslant \text{TOL}$).

(3) Bisect all elements for which the error estimate exceeds the tolerance.

(4) For each of the subdivided elements, solve the *local problem* (2.17) (using the Petrov–Galerkin methods locally) with the known nodal values imposed as local boundary conditions.

(5) Using estimate (2.33), again determine which of the new elements need further refinement.

(6) If elements exist for which $\|e^h\|_{L^\infty(K)} \geqslant \text{TOL}$, bisect them and go to step (4); otherwise, if $\|e^h\|_{L^\infty(K)} < \text{TOL}$ for all elements k, stop the process.

Obviously, other error norms such as those in (2.31) could be used in this refinement strategy. It is important to note that only one equation with one unknown need be solved for the addition of each new nodal point; it is not necessary to resolve the problem globally on the full mesh with each refinement.

2.4. *The Characteristic Adaptive Petrov–Galerkin Method*

Once again, let V_h denote the finite-dimensional space of finite element trial functions spanned by the usual piecewise linear hat functions ψ_i and let $\hat{V}_h$ denote the space of optimal test functions corresponding to V_h. Because our scheme is to be adaptive, the dimension of V_h (and $\hat{V}_h$) will generally change at each time step; and test functions $\hat{v}_h$ in $\hat{V}_h$ are chosen so that

$$\int_0^1 (\varepsilon \Delta t w_x^k \hat{v}_{hx}^k + w^k \hat{v}_h^k + w^k v_h^k)\, dx = \int_0^1 w_x^k v_{hx}^k\, dx, \qquad \forall w^k \in V. \tag{2.34}$$

Our Characteristic Petrov–Galerkin (CPG) Method is defined by the following system of discrete problems:

Find $w_h^k(x) \in V_h \subset H^1(0, 1)$ such that

$$\int_0^1 w_h^k \hat{v}_h\, dx + \varepsilon\, \Delta t \int_0^1 w_{hx}^k \hat{v}_{hx}\, dx$$

$$= \Delta t \int_0^1 f(x, t_k)\, \hat{v}_h\, dx + \int_0^1 w_h^{k-1}(X_h(x, t_k; t_{k-1}))\, \hat{v}_h(x)\, dx, \qquad \forall \hat{v}_h \in \hat{V}_h, \tag{2.35}$$

$$w_h^k(0) = a(t_k),\ w_h^k(1) = b(t_k);$$

w_h^{k-1} being the approximate solution at the previous time-step if $k > 1$ and the initial data u_0 if $k = 1$.

In the above equations, $X_h(x, t_k; t_{k1})$ is an approximate characteristic drawn backward in the time from the point (x, t_k) and usually obtained by replacing the coefficient $c(x, t)$ in (2.12) by a suitable approximation c_h. Replacing, for instance, $c(x, t)$ by a function piecewise constant both with respect to space an time, X_h

becomes a "broken", piecewise-linear line. For the estimates evaluating the difference between the solutions of the previous time step along the exact characteristic and its approximate, we refer to Pironneau [13].

L^∞-Error Estimates. To estimate the error inherent in the approximation scheme (2.35), we first introduce a set of functions $z^k = z^k(x)$ which represents exact solutions of the discrete elliptic system; i.e., z^k is a solution of the problem:

Find $z^k = z^k(x)$ such that

$$\begin{aligned} &z^k - \varepsilon\, \Delta t\, z^k_{xx} = f(x, r_k)\, \Delta t + w_h^{k-1}(X_h(x, t_k; t_{k-1})), \\ &z^k(0) = a(t^k), \qquad z^k(1) = b(t^k). \end{aligned} \tag{2.36}$$

Clearly,

$$\|u^k - w_h^k\|_{L^\infty(0,1)} \leqslant \|u^k - z^k\|_{L^\infty(0,1)} + \|z^k - w_h^k\|_{L^\infty(0,1)}, \tag{2.37}$$

where $u^k(x) = u(x, t_k)$ is the value of exact solution u evaluated at time t_k. The second term on the right-hand of (2.37) results solely from the approximation with respect to x, and, by use of our adaptive scheme, can be made arbitrarily small. Let us denote it by

$$\|z^k - w_h^k\|_{L^\infty(0,1)} = \mu_k. \tag{2.38}$$

While the integrals appearing in (2.35) are always evaluated using numerical integration procedures, we shall not include in the present analysis a study of errors produces by such numerical quadratures.

To estimate the first term in (2.37), we first introduce the truncation error along the approximated characteristic line X_h,

$$-e^k(x) = (u_t + cu_x)(x, t_k) - \frac{1}{\Delta t}\,(u^k(x) - u^{k-1}(X_h(x, t_k; t_{k-1})). \tag{2.39}$$

Subtracting (2.36) from (2.35) we obtain

$$\begin{aligned} &(u^k - z^k) - \varepsilon\, \Delta t (u^k - z^k)_{xx} \\ &\quad = u^{k-1}(x_h(t_{k-1})) - w_h^{k-1}(x_h(t_{k-1})) + e^k\, \Delta t, \end{aligned} \tag{2.40}$$

which, by a maximum-principle argument, implies

$$\|u^k - z^k\|_{L^\infty(0,1)} \leqslant \|u^{k-1} - w_h^{k-1}\|_{L^\infty(0,1)} + \|e^k\|_{L^\infty(0,1)} \Delta t. \tag{2.41}$$

When combined with (2.37), the last result gives:

$$\begin{aligned} \|u_k - w_h^k\|_{L^\infty(0,1)} \leqslant\ &\|u^{k-1} + w_h^{k-1}\|_{L^\infty(0,1)} \\ &+ \|e^k\|_{L^\infty(0,1)}\, \Delta t + \mu_k. \end{aligned} \tag{2.42}$$

Applying (2.42) recursively over every time-step, we arrive at the estimate

$$\|u^k - w_h^k\|_{L^\infty(0,1)} \leqslant \max_{1 \leqslant j \leqslant k} \|e^j\|_{L^\infty((0,1)\times(0,T))} + k\mu, \tag{2.43}$$

where $\mu = \max_{1 \leqslant j \leqslant k} \mu_j$.

Finally, arguments similar to those in Douglas and Russell [8] show that

$$\|e^k\|_{L^\infty(0,1)} \leqslant c \left\| \frac{\partial^2 u}{\partial \tau^2} \right\|_{L^\infty((0,1)\times(0,T))} \Delta t, \tag{2.44}$$

where $\partial/\partial\tau$ denotes the derivative along the approximated characteristic line.

Using (2.44), we obtain finally

$$\|u^k - w_h^k\|_{L^\infty(0,1)} \leqslant c \cdot \left\| \frac{\partial^2 u}{\partial \tau^2} \right\|_{L^\infty(0,1)} \Delta t + k\mu. \tag{2.45}$$

Remark 2.2. (1) By introducing the truncation error along *the approximate characteristic lines*, we have avoided the use of an estimate involving the difference between the exact characteristic and its approximate (refer to Pironneau [15]). For a piecewise constant approximation c_h of c both with respect to time and space variables, the approximate characteristic is rectilinear and the truncation error (2.39) is exactly the same as in Douglas and Russell [10]. One can, of course, insist on defining the truncation error along the exact characteristic (2.4) which will result in extra terms in the final estimate. Such a procedure is only partially justified since u finally is a solution to the *parabolic problem* and not a hyperbolic problem and, therefore, is not constant along characteristic lines. On the other hand, we always expect the variation of u along either the real or approximate characteristics to be small if ε is small and, indeed, this property is crucial to the success of the method.

(2) Estimate (2.45) indicates that the tolerance μ that one may specify for a given problem should be reflected in the choice of the number k of time steps; the error is bounded by the product $k\mu$, so the larger the k, the smaller the value of μ that should be specified.

(3) Use of a Petrov–Galerkin scheme instead of a Bubnov–Galerkin approch *may result in the loss of L^2-stability* (basically one cannot introduce w_h^k into (2.35) as a special choice for a test function since it does not belong to the space of test functions. An *L^∞-stable scheme* would require the use of a discrete maximum principle which would have to take into account specific integration formulas being used. In the next section, we propose an alternative technique which practically solves this problem—the idea of *numerically optimal test functions.*

3. An Alternative Technique—Numerically Optimal Test Functions

In theory, the standard Bubnov–Galerkin method can be used to solve convection-dominated parabolic problems such as (2.1) provided a very fine mesh is used.

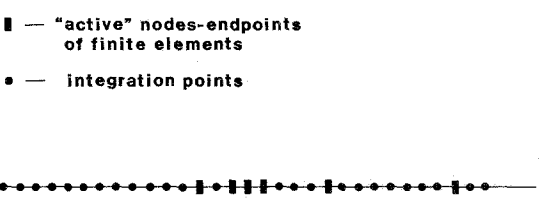

FIG. 3. Illustration of a constant set of integration points.

For instance, it is well known that the Bubnov–Galerkin method combined with the method of characteristics applied to (2.1) can yield good results when the mesh size h, is of the same order as the "viscosity" constant ε. For $\varepsilon = 0.001$, this suggests that one might need 1000 elements to produce reasonable numerical solutions to (2.1): the high computational effort can be avoided by using a special adaptive solver resulting from the Petrov- Galerkin method discussed in the previous section.

The concept of numerically optimal test functions we present in this section is a straightforward generalization of the method presented previously in which integrals appearing in the load equation are evaluated by numerical quadratures over a fixed set of integration points. The idea is to introduce at the onset a fixed uniformly distributed set of integration points and a corresponding trapezoidal integration rule. When adaptive process proceeds, the location of integration points remain unchanged and therefore smaller elements will contain a smaller number of integration points (see Fig. 3).

The integration points define an acceptable fine-mesh Bubnov-Galerkin approximation of the elliptic problem. Introducing a "large" but finite-dimensional subspace W of $H^1(0, 1)$ corresponding to the fine-mesh finite element grid, we accept the following "semi-exact" solution of the following model problem:

Find $\bar{u} \in W$ such that

$$\int_0^1 \bar{u}\bar{v}\, dx + \varepsilon \int_0^1 \bar{u}_x \bar{v}_x\, dx = \int_0^1 f\bar{v}\, dx, \qquad \forall \bar{v} \in W. \tag{3.1}$$

In the above, f can be identified with its L^2-projection onto W or with its interpolant at integration points. Thus, neglecting the difference between the exact solution u and its fine-mesh approximation $\bar{u}$ we shall try to develop a method whose ultimate goal is to reproduce u using the ideas presented in the preceding section.

Toward this end, we start with a much smaller subspace of W, say V_h, and intend to solve (3.1) with a Petrov Galerkin method of the form:

Find $u_h \in V_h$ such that

$$\int_0^1 u_h \hat{v}_h\, dx + \varepsilon \int_0^1 u_{hx} \hat{v}_{hx}\, dx = \int_0^1 f\hat{v}_h\, dx, \qquad \forall \hat{v}_h \in \hat{V}_h. \tag{3.2}$$

Here the $\hat{v}_h$ denote optimal test functions, spanning $\hat{V}_h$ but this time being taken

from the large finite space W instead of H_0^1. It is easily seen that all the ideas discussed in the previous sections are perfectly adaptive to this finite-dimensional case. The critical point is that the optimal test functions in this finite-dimensional case, which we refer to as *the numerically optimal test functions*, are not interpolants of the continuous optimal test functions, and therefore different results for both types of test functions are expected.

Following the plan of Section 2 and 3, we now record the basic results in the context of the finite dimensional space W.

Definition of optimal test function $\hat{v}_h$:

Find $\hat{v}_h \in W$, such that

$$\int_0^1 \psi \hat{v}_h \, dx + \varepsilon \int_0^1 \psi_x \hat{v}_{hx} \, dx = \int_0^1 \psi_x v_{hx} \, dx, \qquad \forall \psi \in W. \tag{3.3}$$

Orthogonality condition ($\bar{u} \in W$):

$$\int_0^1 (\bar{u} - u_h)_x \, v_{hx} \, dx = 0, \qquad \forall v_h \in V_h. \tag{3.4}$$

Optimal error estimate ($\bar{u} \in W$):

$$\|\bar{u} - u_h\|_{H^1(0,1)} \leqslant \|\bar{u} - v_h\|_{H^1(0,1)}, \qquad \forall v_h \in V_h. \tag{3.5}$$

The "extra-superconvergence" result ($\bar{u} \in W$):

$$\bar{u} = u_h \qquad \text{at nodes.} \tag{3.6}$$

Definition of local numerically optimal test functions:

$$\begin{gathered} \psi_i(x_j) = \delta_{ij}, \\ \int_0^1 \psi \psi_i \, dx + \varepsilon \int_0^1 \psi_x \psi_{ix} \, dx = 0, \qquad \forall \psi \in W, \ \psi(x_j) = 0 \end{gathered} \tag{3.7}$$

and

the localization result:

$$\hat{V}_h = \operatorname{span}\{\psi_i\}. \tag{3.8}$$

Even error estimate (2.33) has its discrete counterpart:

$$\|\bar{e}_h\|_{L^\infty(K)} \leqslant \left(\frac{x_k - x_{k-1}}{\varepsilon} \right)^{1/2} (1/\sqrt{\lambda_1}) \, \|L\bar{e}_h\|_{L^2(K)}, \tag{3.9}$$

where $\bar{e}_h$ is the error between "semi-exact" and approximate solutions $\bar{e}_h = \bar{u} - u_h$, and L is a matrix associated with the system of equations resulting from

$$\int_{x_{k-1}}^{x_k} e_h v \, dx + \varepsilon \int_{x_{k-1}}^{x_k} e_{hx} v_x \, dx = \int_{x_{k-1}}^{x_k} (f - u_h) v \, dx, \qquad \forall v \in W,\ v(x_{k-1}) = v(x_k) = 0, \tag{3.10}$$
$$e_h(x_{k-1}) = e_h(x_k) = 0,$$

and λ_1 denotes the smallest eigenvalue of L which, this time, must be evaluated numerically.

Remark 3.1.

(1) The two norms in (3.9) are defined on the finite dimensional space W where any two norms are equivalent and therefore the constant in estimate (3.9) can be evaluated directly by solving a corresponding minimization problem.

(2) The discrete form of our method discussed here for one-dimensional problems can be generalized to multidimensional problems in a straightforward manner. We hope to report some extensions to two-dimensional cases in a forthcoming paper.

(3) In estimate (3.9), f is to be identified with its L^2-projection onto W or its interpolant at integration points.

Returning to problem (3.1), our discrete method with numerically optimal test functions leads to the following scheme for the diffusion step in our algorithm for convection-diffusion problems:

For $k = 1, 2, \ldots, K$, find $w_h^k \in V_h \subset W$ such that

$$\int_0^1 w_h^k \hat{v}_h \, dx + \varepsilon \, \Delta t \int_0^1 w_{hx}^k \hat{v}_{hx} \, dx$$
$$= \Delta t \int_0^1 f(t_k) \, \hat{v}_h \, dx + \int_0^1 w_h^{k-1}(X_h(x, t_k; t_{k-1})) \, \hat{v}_h \, dx, \tag{3.11}$$
$$\forall \hat{v}_h \in \hat{V}_h \subset W,$$
$$w_h^k(0) = a(t^k), \qquad w_h^k(1) = b(t^k).$$

Due to the adaptive character of the method, both V_h and $\hat{V}_h$ here may change at every time-step, but both remain subspaces of the larger space W.

We will not reproduce here error estimates for the standard Bubnov–Galerkin method combined with the method of characteristics (see Pironneau [15], or Douglas and Russell [10]). We note that by using our adaptive technique with numerically optimal test functions we can reproduce the standard Bubnov–Galerkin results with a given, arbitrary small tolerance μ possibly saving in this

way many unnecessary degrees of freedom and never solving large systems of equations. Indeed, the bisecting solution technique involves the solution of only one equation for each local problem. With sufficiently small μ, we may activate all nodes this recovering the "semi-exact" solution on the fine mesh. Thus the method can be interpreted as a very special and effective solver of the implicit diffusion step in the standard Bubnov–Galerkin method for possibly very large systems of equations.

There are several other advantages of such an approach. The source term $f(t_k)$ on the right-hand side in (3.11) need be evaluated only once (due to the fact that number and location of the integration points remain unchanged); for a uniform distribution of points, the method can be directly compared with finite difference techniques (a useful feature in studying hyperbolic problems in the next section) and, finally, the concept results in an L^2-stable scheme.

To confirm this last assertion, let us denote by u^k the semi-exact solution to (2.1) obtained with the fine-mesh Bubnov–Galerkin method. Assuming that the method is L^2-stable (refer to Pironneau [15]), one has for $f \cong 0$,

$$\|u^k\|_{L^2(0,1)} \leqslant \|u^{k-1}\|_{L^2(0,1)}. \tag{3.12}$$

Denoting by z^k solution of a typical time-step but with initial data w_h^{k-1} chosen instead of u^{k-1}, from the L^2-stability and linearity of the problem follows also that

$$\|u^k - z^k\|_{L^2(0,1)} \leqslant \|u_h^{k-1}\|_{L^2(0,1)}. \tag{3.13}$$

Thus,

$$\begin{aligned} \|u_k - w_h^k\|_{L^2(0,1)} &\leqslant \|u^k - z^k\|_{L^2(0,1)} + \|z^k + w_h^k\|_{L^2(0,1)} \\ &\leqslant \|u^{k-1} - w_h^{k-1}\|_{L^2(0,1)} + \mu. \end{aligned} \tag{3.14}$$

When applied recursively at every time step yields, we get

$$\|u^k - w_h^k\|_{L^2(0,1)} \leqslant k\mu. \tag{3.15}$$

It follows that for a given number of time-steps, we may choose μ small enough to recover the semi-exact solution with a required tolerance.

Finally, we note that our scheme is "almost" L^2-stable, since (3.12) yields:

$$\begin{aligned} \|w_h^k\|_{L^2(0,1)} &\leqslant \|w_h^k - z_h^k\|_{L^2(0,1)} + \|z_h^k\|_{L^2(0,1)} \\ &\leqslant \mu + \|w_h^{k-1}\|_{L^2}. \end{aligned} \tag{3.16}$$

Numerical experiments discussed in Section 6 confirm the step-wise stability estimate (3.16). Since the discrete version of the method is L^2-stable in this sense, it may be desirable to replace (3.9) by a local L^2-estimate.

4. Application to Certain Nonlinear Hyperbolic Problems

In general, only distributional solutions of nonlinear hyperbolic problems may exist for all $t \geqslant 0$, and these solutions may not be uniquely determined by the initial data (see, e.g., Lax [13]). One thus seeks to determine which of these distributional solutions is physically reasonable, in the sense that it corresponds to a positive production of entropy across of discontinuity of the solution. Such "entropy solutions" are uniquely determined by the initial conditions for the scalar one-dimensional case, and they are usually identified with limits of dissipative solutions of a parabolic regularization of the given hyperbolic problem as the dissipation tends to zero. Thus, to obtain entropy solutions of the nonlinear hyperbolic problem of the type

$$\begin{aligned} u_t + \sigma(u)_x &= 0, \qquad x \in \mathbb{R},\ t > 0, \\ u(x, 0) &= u_0(x). \end{aligned} \tag{4.1}$$

Where the flux $\sigma(u)$ is a nonlinear function of u, it is customary to consider a related parabolic problem, such as

$$\begin{aligned} u^\varepsilon_t + \sigma(u^\varepsilon)_x - \varepsilon u^\varepsilon_{xx} &= 0, \qquad x \in \mathbb{R},\ t > 0, \\ u^\varepsilon(x, 0) &= u_0(x), \end{aligned}$$

and to achieve an entropy solution u to (4.1) as a limit $u^\varepsilon \to u$, in some sense, as $\varepsilon \to 0$.

With these ideas in mind, we consider the following nonlinear parabolic problems:

$$\begin{aligned} &u_t + \sigma(u)_x - \varepsilon u_{xx} = 0, \qquad 0 < x < q,\ t > 0, \\ &u(0, t) = a(t),\ u(1, t) = b(t), \qquad t \geqslant 0, \\ &u(x, 0) = u_0(x). \end{aligned} \tag{4.3}$$

Conceivably, by applying our CGP-method to (4.3) and taking ε sufficiently small, we could arrive at reasonable numerical solutions to certain classes of nonlinear hyperbolic problems.

Toward this end, we consider once again Petrov–Galerkin approximations of elliptic systems:

Find $w^k_h(x) \in V_h$ such that

$$\begin{aligned} &\int_0^1 w^k_h \hat{v}_h \, dx + \varepsilon \, \Delta t \int_0^1 w^k_{hx} \hat{v}_{hx} \, dx \\ &\quad = \int_0^1 w^{k-1}_h (X_h(x, t_k; t_{k-1})\, \hat{v}_h(x) \, dx, \qquad \forall \hat{v}_h \in \hat{V}_h, \end{aligned} \tag{4.4}$$

$$w^k_h(0) = a(t_k), \qquad w^k_h(1) = b(t_k).$$

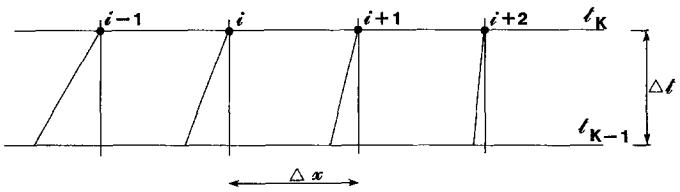

FIG. 4. Construction of characteristics.

The essential difference between this case and that discussed previously is that the characteristic lines are now solution-dependent.

With the fractional step method-notation in use, we may split (4.4) into two steps:

Transport:

$$w_h^{k-1/2}(x) = w_h^{k-1}(X_h(x, t_k; t_{k-1})). \tag{4.5}$$

Diffusion:

$$\begin{gathered}\int_0^1 w_h^k \hat{v}_h \, dx + \varepsilon \, \Delta t \int_0^1 w_{hx}^k \hat{v}_{hx} \, dx = \int_0^1 w_h^{k-1/2} \hat{v}_{hx} \, dx, \qquad \forall \hat{v}_h \in \hat{V}_h, \\ w_h^k(0) = a(t_k), \qquad w_h^k(1) = b(t_k).\end{gathered} \tag{4.6}$$

Several schemes for constructing approximate characteristic lines suggest themselves. We continue to employ the numerically optimal test functions and, for simplicity, we shall approximate characteristic by straight lines within each time step (Fig. 4). Of course, in the pure hyperbolic case the characteristic lines are, in fact, straight lines, so that for small ε this linear approximation seems to be a reasonable way to approximate the transport step in the algorithm. This is contrary to the use of the method of characteristics in the context of Navier-Stokes equations (see, e.g., Huffenus and Khaletzky [11]), where, with higher order Runge–Kutta procedures in use, the characteristics are never rectilinear, even for small ε.

By constructing characteristic lines backward in time at every integration point, we arrive at the method illustrated in Fig. 4. Suppressing the h index for clarity, we have,

$$w_i^{k-1/2} = \begin{cases} w_i^{k-1} - \lambda c_i (w_i^{k-1} - w_{i-1}^{k-1}) & \text{if } c_i \geqslant 0 \\ w_i^{k-1} - \lambda c_i (w_{i+1}^{k-1} - w_i^{k-1}) & \text{if } c_i \leqslant 0, \end{cases} \tag{4.7}$$

where $\lambda = \Delta t / \Delta x$, and c_i characterize the slope of characteristics. These slopes can be calculated in three ways. Denoting $A(u) = \sigma'(u)$, we may use:

Explicit scheme:

$$c_i = A(u_i^{k-1}). \tag{4.8}$$

Semi-implicit scheme:

$$c_i = A(u_i^{k-1/2}). \tag{4.9}$$

Fully-implicit scheme;

$$c_i = A(u_i^k). \tag{4.10}$$

Scheme (4.9) is referred to as semi-implicit scheme since, upon substituting it to (4.7), one can still solve (4.7) explicitly for $w_i^{k-1/2}$. Only the last fully implicit scheme couples the two fractional steps of our method and results in a nonlinear scheme requiring extra iterations. Without going into algebraic details, we record some simple observations:

(1) The requirement that characteristic lines should never exceed the neighboring "cell," results in the limitation of the time step in the form of the usual CFL-condition.

(2) Both schemes (4.8) and (4.9) are monotone (see, e.g., Crandall and Majda [8]) under some additional limitations on time-step Δt, with much weaker limitations needed in the case of the semi-implicit scheme.

(3) None of the schemes is in a conservation form.

In our numerical experiments, we have restricted ourselves to the implicit schemes.

Finally, we note that it is not difficult to derive error estimates for these schemes similar to those in Douglas and Russel [10]. However, since such estimates would reflect more the parabolic than the hyperbolic nature of the problem, their applicability to the problem seems to be of questionable value.

5. Numerical Experiments

5.1. *Some Computational Details*

We shall now describe the results of several numerical experiments performed using our method. All results were obtained using the notion of "numerically" optimal test functions discussed in Section 3.

We shall assume that the integration points are fixed, uniformly distributed and that the integration is performed by using the simplest trapezoid formula. The total number of integration points is chosen in such a way that the corresponding fine-mesh distance is of the range of the constant assumed in all the examples.

Suppose now that we start with a uniform mesh of n elements and a predicted maximum number of mesh refinements (bisections) equal k. Since the smallest elements must have at least two integration points (which coincide with their endpoints) the number of integration points is:

$$N = n2^k + 1. \tag{5.1}$$

If k is equal, for instance, to 6 in the mesh refinement procedure, we deal with elements consisting of 65, 33, 7, 9, 5, 3, and finally 2 integration points. For each of such elements the corresponding minimal eigenvalues (recall (3.9)) necessary for error estimates and numerically optimal test functions are determined just once, before running the program, which is possible under the assumption that time step Δt is constant. The stored eigenvalues and test functions are then used at every time step.

5.2. *Model Elliptic Problem*

As a test of our elliptic solver, problem (2.17) is solved with a right-hand side f and boundary conditions corresponding to the following exact solution:

$$u(x) = -\exp(-x) - \exp[(1+\varepsilon)(x-1)/\varepsilon] + (A-B)x - A \tag{5.2}$$

with constants A and B chosen so that

$$u(0) = u(1) = 0. \tag{5.3}$$

For small ε, the solution (5.2) possesses a thin boundary-layer near $x = 1$. The numerical data have been chosen as follows:

$$\text{Number of integration points} \quad N = 10 \cdot 2^6 + 1,$$

$$\varepsilon = 0.01,$$

$$L^\infty\text{-error tolerance} \quad \text{TOL} = 0.0001.$$

Figure 5 presents both numerical and exact solutions (with the scale used they are indistinguishable) and the resulting optimal finite element mesh for 50 elements.

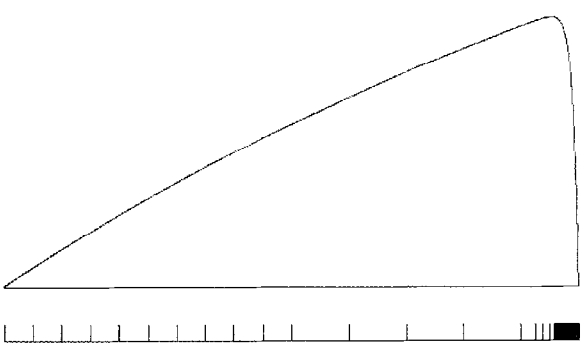

FIG. 5. Model elliptic problem–solution and the optimal finite element mesh.

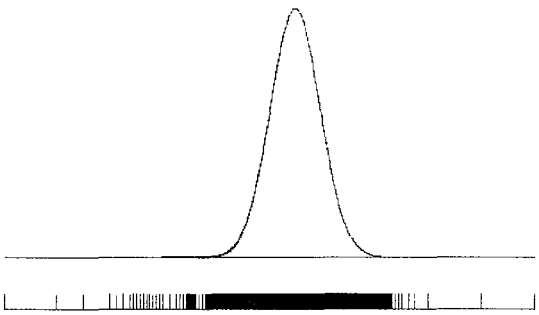

FIG. 6. Convection-dominated problem–solution and the mesh at $t = 0.15$.

5.3. *Convection-dominated Parabolic Equation*

As a test for the convection-diffusion scheme for problem (2.1), we follow Donea *et al.* [9] and consider a problem for which the solution is a Gaussian profile translating and spreading in time of the form

$$u(x, t) = (2\varepsilon\bar{t})^{-1/2} \exp[-(x-\bar{t})^2/4\varepsilon\bar{t}], \tag{5.5}$$

where $\bar{t} = t + 0.4$ with a variable advection velocity,

$$c(x, t) = 2[\tan^{-1}(x - x_0)/\pi][1 - \exp(-(t+0.2)/0.2)]. \tag{5.6}$$

Since u is the exact solution for $x \equiv 1$ the source term has to be calculated as $f(x, t) = [c(x, t) - 1]\, u_x(x, t)$. The numerical data are as follows:

Number of integration points $N = 10 \cdot 2^6 + 1$,

$\varepsilon = 0.002$,

tolerance $\quad \mathrm{TOL} = 0.001$,

time-step $\quad \Delta t = 0.0015$,

$x_0 = 0.5$,

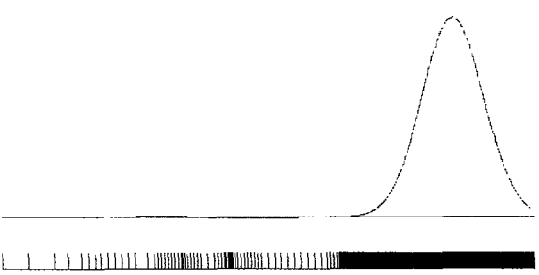

FIG. 7. Convection-dominated problem–solution and the mesh at $t = 0.45$.

Figures 6 and 7 illustrate both the exact solution and the calculated solution at times $t=0.15$ (after 100 iterations) and $t=0.45$ (after 300 iterations). Three hundred time steps were calculated. The characteristics are approximated by broken lines (which corresponds to the approximation of function c by piecewise constant functions, both with respect to space and time variables) and with the Δt chosen so that they never exceed a neighboring cell. A larger choice of Δt results in the approximation of characteristics by broken lines identical with those described, e.g., in Pironneau [15], which according to our experiments, produces a deterioration in the quality of the solution, especially in the case of very irregular solutions. In our particular formulation, it is not necessarily computationally efficient to use large time-steps since the approximation of characteristic lines over large time-steps may be expensive.

5.4. *Bürger's Equation—Regular Solution*

As a final problem, we consider the Bürger's equation

$$u_t=(\tfrac{1}{2}u^2)_x-\varepsilon u_{xx}=0 \tag{5.8}$$

with the boundary and initial data corresponding to the exact N-wave solution (see Lohar and Jain [14]),

$$u(x,t)=\frac{x/\bar{t}}{1+\exp(x^2/4\varepsilon\bar{t})(\bar{t}/t_0)^{1/2}}, \tag{5.9}$$

where $\bar{t}=t+1$. Following Lohar and Jain [14], we choose

$$t_0=\exp(1/8\varepsilon). \tag{5.10}$$

The remaining numerical data are as follows:

Number of integration points $N=10\cdot 2^6+1$,

$\varepsilon=0.01$,

tolerance $\mathrm{TOL}=0.00005$,

time-step $\Delta t=0.0015$.

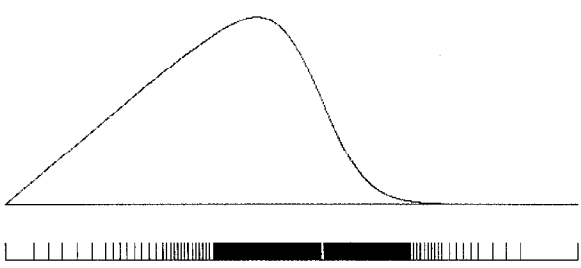

FIG. 8. Bürgers' equation–N-wave solution at $t=0.15$.

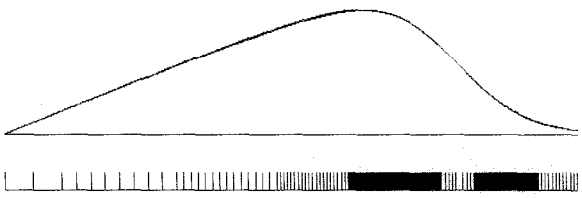

FIG. 9. Bürgers' equation–N-wave solution at $t = 1.5$.

Numerical results are presented in Figs. 8 and 9, for times $t = 0.15$ and $t = 1.5$ where numerical results are seen to be indistinguishable from the exact solution. At $t = 1.5$, after 1000 iterations, a slightly overdiffusive character of the approximation emerges as a result of numerical dissipation. In the program used in these calculations, the fully implicit construction of characteristics (recall (4.8)), required a maximum of

tolerance, TOL. The semi-implicit scheme gives, within the range of 1000 steps considered, results indistinguishable for the exact solution. The total number of elements varies with time but never exceeded 240 elements. Of course, by setting a large tolerance we get a smaller number of elements, but the quality of the solution may deteriorate due to the discrete stability property characterized by (3.16).

5.5. *Bürger's Equation—Discontinuous Solution*

We conclude our numerical examples with an analysis of Eq. (5.8), this time with boundary and initial data corresponding to the solution:

$$u(x, t) = \begin{cases} 1 & \text{if } x < 0.4 + 0.5t \\ 0 & \text{otherwise.} \end{cases} \tag{5.11}$$

Solution (5.11) is discontinuous and independent of ε and is only formally a solution to (5.8). In fact, (5.11) is a classical shocklike solution to (5.8) but with $\varepsilon = 0$: the so-called Riemann problem (see, e.g., Lax [13]). Therefore only for small

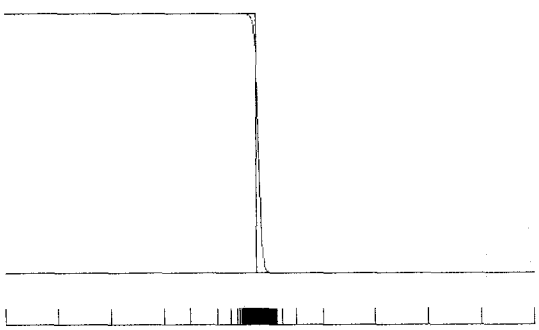

FIG. 10. Bürgers' equation–shock at $t = 0.15$.

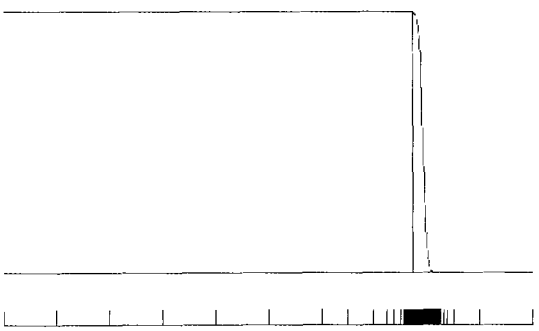

FIG. 11. Bürgers' equation–shock at $t = 0.75$.

ε's (recall the remarks at the beginning of Sect. 3) can we expect a numerical solution to approach the exact one at a reasonable rate. With numerical data chosen as:

$$\text{Number of integration points} \quad N = 10 \cdot 2^6 + 1,$$

$$\varepsilon = 0.0015,$$

$$\text{tolerance} \quad \text{TOL} = 0.00005,$$

$$\text{time-step} \quad \Delta t = 0.0015,$$

the numerical results at $t = 0.15$ and $t = 0.75$ are those presented in Figs. 10 and 11. As one can see, the numerical shock travels with a slightly greater velocity than the exact solution.

6. CONCLUDING COMMENTS

As will be shown in subsequent work, there are many problems this paper leaves unsolved. The concept of numerically optimal test functions makes it possible to generalize most of the results of the present paper to multidimensional cases. Still, the main limitation of the present version of our method is the fact that the method's accuracy is limited by that the characteristic Bubnov–Galerkin method on the fine grid. This restricts possible applications to moderately small viscosity parameters ε only, as has been reflected in the numerical examples in the preceding section.

The question of how to deal with the case of very small ε's (say of order 10^{-6}) is one of the possible directions in which generalizations might be sought.

By introducing successively finer fine-grid approximations into the adaptive strategy, it may be possible to push the method to cases in which ε is very small. Such generalizations may also involve strategies in which the number and location of grid points can vary with each time-step. These and other possibibilities require additional study.

ACKNOWLEDGMENTS

The work reported here was completed under the support of a subcontract to NASA Langley Research Center, Contract NAS1-17894, through Lockheed Missile and Space Co., Huntsville, Alabama.

REFERENCES

1. I. BABUSKA AND W. RHEINBOLDT, *Siam J. Numer. Anal.* **15**, 736 (1978).
2. I. BABUSKA AND W. RHEINBOLDT, *Math. Comput.* **33**, 435 (1979).
3. J. W. BARRET AND K. W. MORTON, *Comp. Meth. Appl. Mech and Engng.* **46**, 97 (1984).
4. M. BIETERMAN, in *Proceedings of Aadaptive Methods and Error Refinement in Finite Element Computation, Lisbon*, edited by Babuska *et al.* (Wiley, London, to appear).
5. M. BIETERMAN AND I. BABUSKA, *Numer. Math.* **40**, 339 (1982).
6. M. BIETERMAN AND I. BABUSKA, *Numer. Math.* **30**, 373 (1982).
7. M. BIETERMAN AND I. BABUSKA, "An Adaptive Method of Lines with Error Control for Parbolic Equations of the Reaction–Diffusion Type," Univ. of Maryland, 1984 (unpublished).
8. M. G. CRANDALL AND A. MAJDA, *Math. Comput.* **34** (149), (1980).
9. J. DONEA, S. GULLIANI, H. LAVAL AND L. QUARTAPELLE, *Comput. Methods Appl. Mech. and Eng.* **45**. 123 (1984).
10. J. DOUGLAS AND T. T. RUSSELL, *SIAM J. Numer. Anal.* **19** (5), 871 (1982).
11. J. P. HUFFENUS AND D. KHALETZKY, *Int. J. Numer. Meth. Fluids* **4**, 247 (1984).
12. T. J. R. HUGHES, "A Short-Capturing Finite Element Method," Stanford Univ., 1984 (unpublished).
13. P. D. LAX, *Hyperbolic System of Conservation Laws and the Mathematic Theory of Sock Waves* (Society for Industrial and Applied Mathematics, Pennsylvania, 197).
14. B. L. LOHAR AND P. C. JAIN, *J. Comput. Phys.* **39**, 433 (1981).
15. O. PIRANNEAU, *Numer. Math.* **38**, 309 (1982).
16. G. STRANG AND G. J. FIX, *An Analysis of the Finite Element Method* (Prentice–Hall, Englewood Cliffs, N. J., 1973).
17. W. G. SZYMCZAK, in: *Proceedings of Adaptive Methods and Error Refinement in Finite Element Computation, Lisbon* (edited by Babuska *et al.*) (Wiley, London, to appear).
18. W. G. SZYMCZAK AND I. BABUSKA, *SIAM J. Numer. Anal.* **21**, 910 (1984).